Modeling of Materials Behavior of HIP Superalloys for Liquid Rocket Engine Turbopump Applications

K.O. Lee*, K.H. Bae*, S.B. Lee*, S.H. Yoon**, S.M. Jeon** and J. Kim**
*Department of Mechanical Engineering, Korea Advanced Institute of Science and Technology,
373-1 Guseong Dong, Yuseong Gu, Daejeon, 305-701, South Korea.
**Turbopump Department, Korea Aerospace Research Institute,
45 Eoeun Dong, Yuseong Gu, Daejeon, 305-333, South Korea.

Abstract
Development of high power and light weight liquid rocket engine is essential for implementing space launch vehicle. To achieve the high ratio of thrust to weight, most liquid rocket engines use turbopumps, which pressurize fuels and oxidizers, and hot gas driven turbine rotors are usually used to operate the whole turbopump system. Therefore, it is considered to be very important to predict material behaviors at elevated temperatures for the design and manufacturing of reliable turbopump system. Hot isostatic pressing (HIP) is one of the promising manufacturing methods for gas turbine rotors. In this research, four superalloys, forged and HIPed Inconel 718, HIPed Rene 95, and HIPed Astroloy, were investigated at elevated temperatures. Serrated flow induced by dynamic strain aging (DSA) was observed on certain temperature regions, where the embrittlement of the materials progressed. A dislocation barrier model was modified to describe the material behavior including creep relaxation effect at high temperatures. The suggested model was found to predict well the deformation behaviors of the superalloys at elevated temperatures except some DSA regions.

1. Introduction

Development of high power and light weight liquid rocket engine is essential for implementing space launch vehicle. To gain high thrust to weight ratio, most liquid rocket engines use turbopumps that pressurize fuels and oxidizers. Usually hot gas driven turbine rotors are used to rotate the whole turbopump system, therefore it is very important to predict material behaviors at elevated temperatures for the design and manufacturing of reliable turbopump system. To develop reliable turbopump rotors, nickel- and cobalt-based superalloys are used widely. The development of powder processed nickel-base superalloys for gas turbine engine applications has been progressed since 1970s [1]. It was demonstrated that practically unworkable high strength nickel-base superalloys could be made readily forgeable by a combination of rapid solidification and isothermal metalworking technologies [2]. This allowed the production of high strength powder processed discs for high performance turbopump blade (Figure 1). With powder metallurgy technology, high strength alloys are first atomized from the melt into a powder which is subsequently consolidated into fully dense compacts by hot extrusion or hot isostatic pressing (HIP) [1,2]. Consolidation produces compacts which have excellent mechanical properties and can be used in the as-consolidated condition in some applications. The as-consolidated compacts can also be further processed by forging to optimize their mechanical properties.
In this research, four superalloys (Forged Inconel 718, HIPed Inconel 718, HIPed Astroloy, and HIPed Rene 95) were tested at elevated temperatures for developing turbine blisk. To avoid the concentrations of thermal and mechanical stress and thermal fatigue fracture problems, deformation behavior at elevated temperatures should be known and constitutive relation should also be developed. Using the results of the experiments, a physically-based model is developed based on a dislocation kinetics and its applicability is examined.

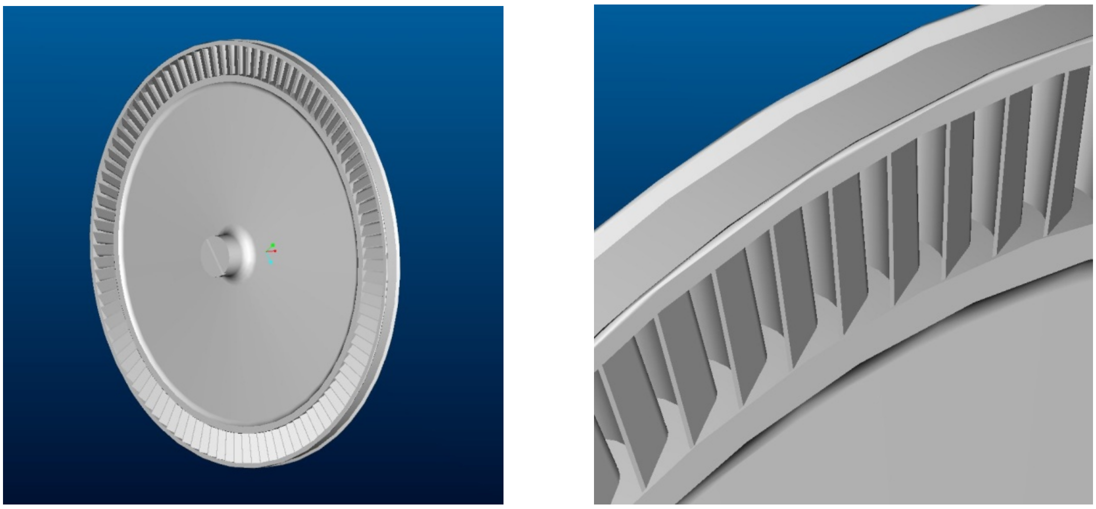

Figure 1: The shapes of turbopump blade

2. Experimental procedure

2.1 Materials and samples

The chemical compositions of Inconel 718, Astroloy, and Rene 95 are given in Table 1. Inconel 718 was manufacutred by both forging with casting Inconel and HIP processing with powder Inconel. Astroloy and Rene 95 were manufactured through HIP process with powders. As-received materials were machined into dog-bone type specimens with a diameter of 6 mm and a gage length of 36 mm in accordance with ASTM E606-92.

Table 1: Chemical compositions of the testing materials (wt,%)

Material	C	B	Zr	W	Co	Ni	Cr	Mo	Al	Ti	Nb	Cu	Fe
Inconel 718	0.08	-	-	-	-	52.5	19	3	0.5	0.9	5.1	0.15	18.5
Astroloy	0.06	0.03	0.06	-	15	56.5	15	5.25	4.4	3.5	-	-	<0.3
Rene95	0.16	0.01	0.05	3.5	8	61	14	3.5	3.5	2.5	3.5	-	<0.3

2.2. Testing methods

Tensile tests were performed at a strain rate of 0.002/s using an MTS hydraulic testing machine in the temperature range of 293 to 1173K. High temperature environment was achieved in air with an induction heating system, which can maintain the testing temperature within ±1K. Temperature was measured using a K-type thermocouple arrangement. The deformation of the specimen was measured by MTS high-temperature uniaxial extensometer. Low temperature tests at 123 and 173K were carried out for Inconel 718 forging material, where liquid nitrogen was used to make low temperature environment.

3. Experimental results

Serrated yielding appeared in the temperature range of 400 to 700℃ (figure 2). Serrations are defined as the repeated and systematic fluctuations of the load, i.e., load drops in the stress-strain curves during plastic deformation [3]. In austenitic stainless steels and nickel alloys, the most widely accepted mechanism of serrated yielding is dynamic strain aging during plastic deformation as a result of the interaction between solute atoms and mobile dislocations. Hale et al. [4] reported serrated flows in Inconel 719SPF, and it was attributed to the diffusion of an interstitial solute such as carbon in the temperature range of 177-525℃ and the diffusion of substitutional atom in higher temperature range of 525-650℃. Dynamic strain aging often generates higher material strength, hence, flow stress of Rene 95 at 600℃ becomes higher than those at other temperatures (Figure 2(b)). Also, flow stress developed is lowered beyond 800℃.

The experimental results and the references [5-6] reveal the following characteristics for superalloys: (1) the plastic flow stress of the materials is both temperature- and strain rate-dependent; (2) dynamic strain aging occurs at the strain rate of 0.002/s in the temperature range of 200-700℃ and its degree becomes weaker with increasing strain rate or beyond 700℃; (3) stress relaxation takes place beyond 700℃ due to climbing of dislocations and this causes the flow stress developed to lower.

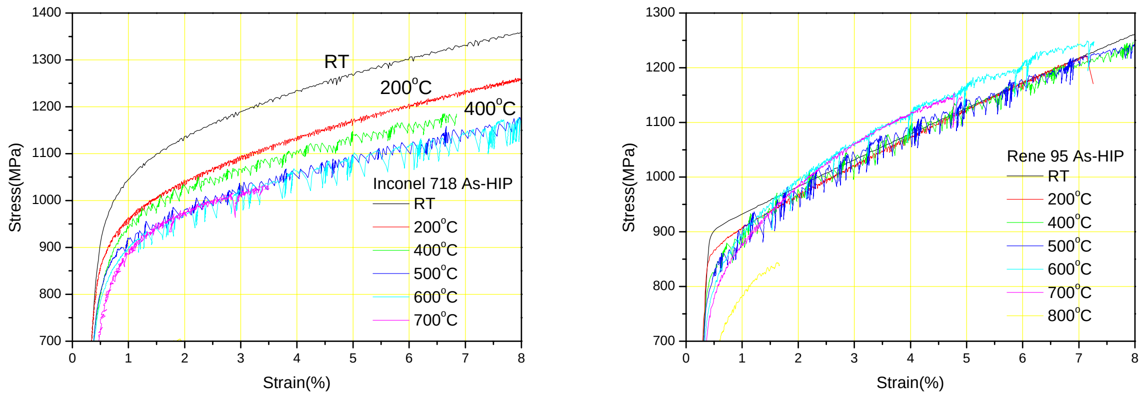

(a) (b)

Figure 2: Stress and strain curves of (a) Inconel 718 made by HIP, (b) Rene 95 made by HIP. Serrations appeared in various kinds of temperautres such as from 400℃ to 700℃.

4. Constitutive modeling

4.1 Compositions of flow stress

In this research, a suitable constitutive model for these superalloys which include all the above effects was developed. Based on the dislocation energy barrier model suggested by Kocks et al.[7], and guided by experimental results, a physically based model has been developed by Nemat-Nasser and Isaacs[8] and Nemat-Nasser and Guo [9] and applied to several polycrystalline metals. A similar model which includes all the characteristics observed in superalloys does not exist. In the present work, we seek to incorporate the experimental understanding described earlier for Inconel 718 and other materials into the constitutive model suggested by Nemat-Nasser and co-workers [8,9]. Also, creep relaxation effect was included in the high temperature range above 800℃.
Consider the plastic flow in the range of temperature and strain rate, where diffusion and creep are not dominant, and the deformation occurs basically by the motion of dislocations. For many materials, it can be assumed the flow stress, τ, consists of two stress terms: one is essentially due to the short-range thermally activated effect which may include the Peierls stress, point defects such as vacancies and self-interstitials, other dislocations which intersect the slip plane, alloying elements, and solute atoms (interstitial and substitutional). We denote this as τ^*. The other is the athermal component, τ_a, mainly due to the long-range effects and grain boundaries.
At elevated temperatures, the dynamic strain aging was observed, hence, some researchers included the effect of dynamic strain aging as hardening component of flow stress, τ_D. Also, creep relaxation effects should be added in higher temperatures. The flow stress decreases as the creep effect becomes significant, then, creep relaxation stress part was subtracted from the total flow stress. We denote this by τ_c.

$$\boldsymbol{\tau} = \boldsymbol{\tau}^* + \boldsymbol{\tau}_\mathbf{a} + \boldsymbol{\tau}_\mathbf{D} - \boldsymbol{\tau}_\mathbf{c} \tag{1}$$

For simplicity, however, the dynamic strain aging effect was not considered in this present study. That is, $\tau_D \approx 0$.

4.2 Athermal stress component, τ_a.

The athermal part, τ_a, of the flow stress is independent of strain rate, $\dot{\gamma}$. Here the temperature effect on τ_a is only through the temperature dependence of the elastic modulus, especially the shear modulus, $\mu(T)$ [9]. τ_a mainly depends on the microstructure of the material such as the dislocation density, grain size, point defects, and various solute atoms. Based on linear elasticity, τ_a would be proportional to $\mu(T)$. Therefore,

$$\boldsymbol{\tau_a = f(\rho, d_G, \dots)\mu(T)/\mu_0} \qquad \textbf{(2)}$$

where ρ is the average dislocation density, d_G is the average grain size, the dots stand for parameters associated with other impurities, and μ_0 is the reference value of the shear modulus. In most cases, strain γ increases monotonically and defines the loading path. Nemat-Nasser and Guo [9] expressed this parameter as load parameter to define the variation of dislocation density, the average grain size, and other parameters which affect athermal stress component. This can be approximated as power law relationship like Ramberg-Osgood equation.

$$\boldsymbol{\tau_a = \tau_a^0\, \gamma^n} \qquad \textbf{(3)}$$

where a_1 and n are free parameters which should be determined experimentally. We emphasize that the effective plastic strain, γ, or any plastic-strain components cannot in general represent the microstructure, and here γ is used strictly as a load parameter. To identify the constitutive parameters for the athermal stress in Eq. (3), we examined the variation of the flow stress with temperature, as shown in Figure 2. Nemat-Nasser and Issac [8] showed that certain critical value of the temperature, in which flow stress is essentially independent of the temperature, is 430K at the strain rate of 10^{-3}/s and 1000K at the strain rate of 5000/s. In this study, we assumed that at the strain rate of 2×10^{-3}/s, the critical temperature (i.e., T_c) is 673K in Inconel 718 materials and 573K in both Astroloy and Rene 95. Therefore, the parameters τ_a^0 and n can be calculated at the critical temperature as Table 2.

Table 2: Model parameters for the superalloys.

	τ_a^0(MPa)	n	p	q	T_c (0.2%/s)	$\hat{\tau}$(MPa)	Q_c/k(K)	τ_c^0(MPa)	n'
Inconel 718 forged	1433.1	0.051	2/3	2	673	850	14389	6.86	0.128
Inconel 718 HIP	1330.7	0.069	2/3	2	673	700	9724	21.1	0.118
Astroloy HIP	1171.5	0.06	2/3	2	573	500	14886	0.938	0.044
Rene 95 HIP	1307.2	0.071	2/3	2	573	600	16748	0.551	0.0814

4.3 Thermally activated component of the flow stress,

Kocks et al. [7] suggested the relationship between ΔG and τ^* considering a dislocation gliding in the x direction under a thermal resolved shear stress τ^*, which produces a force τ^*b per unit length on the line. Also, he assumed the spacing of the obstacles along the line is l, so that the applied forward force applied on the line per obstacle result in τ^*bl. To overcome the barrier, the Gibbs free energy of activation is required. The probability of energy ΔG is occurring by thermal fluctuations at temperature T is given by representing a typical barrier encountered by a dislocation:

$$\boldsymbol{\Delta G = G_0[1 - (\tau^*/\hat{\tau})^p]^q} \qquad \textbf{(4)}$$

$$\boldsymbol{G_0 = \hat{\tau} b \lambda l = \hat{\tau} V^*,} \qquad \textbf{(5)}$$

where $0 < p \leq 1$ and $1 \leq q \leq 2$ define the configuration of the short-range barrier, $\hat{\tau}$ is the shear stress above which the barrier is crossed by a dislocation without any assistance from thermal activation, that is, the thermal stress at 0K, and G_0 is the free energy required for a dislocation to overcome the barrier solely by its thermal activation; b is the magnitude of the Burgers vector; λ is the average effective barrier width, and V^* is the activation volume. We note in passing that $l^* = (V^*)^{1/3}$ provides a natural length scale in this physics-based model.

Also, the plastic strain rate is defined as $\dot{\gamma} = b\rho_m\bar{v} = b\rho_m f_0 \exp(-\Delta G/kT)$, where $\bar{v}$ is their average velocity of the dislocation having the attempt frequency of f_0 to overcome the obstacles and k is the Boltzmann constant. From Equations (4) and (5),

$$\boldsymbol{\tau^* = \hat{\tau}\left[1 - \left(\frac{kT}{G_0} \ln\frac{\dot{\gamma}}{\dot{\gamma}_r}\right)^{1/q}\right]^{1/p} \qquad (T \le T_c)} \tag{6}$$

$$\boldsymbol{T_c = \left(-\frac{k}{G_0} \ln\frac{\dot{\gamma}}{\dot{\gamma}_r}\right)^{-1}} \tag{7}$$

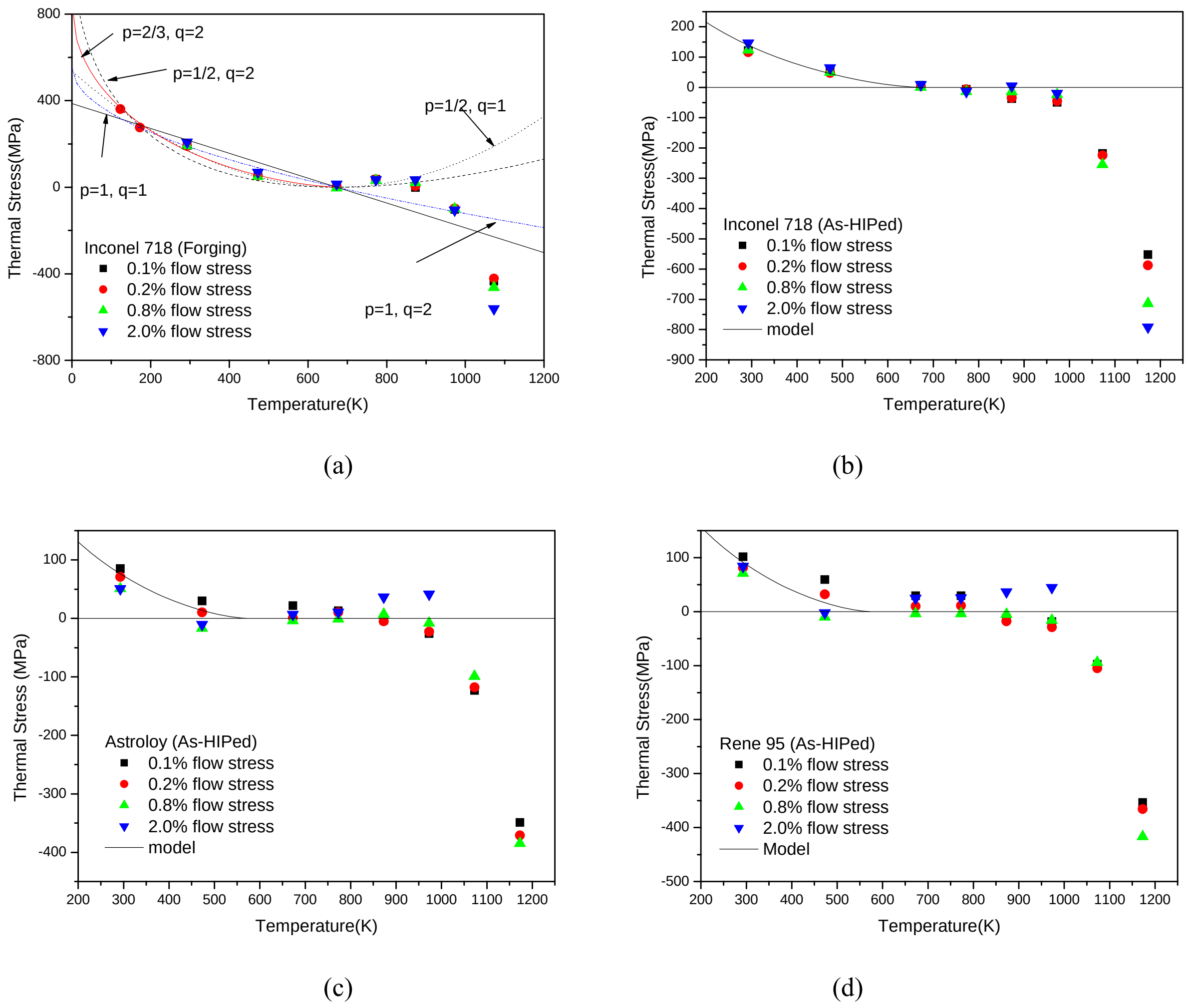

Figure 3: The variations of thermal stresses of superalloys with temperature: (a) Inconel 718 made by forging, (b) Inconel 718 made by HIP, (c) Astroloy made by HIP, and (d) Rene 95 made by HIP

In Equation (6), the parameters p and q depict the profile of the short-range energy barrier to the motion of dislocations. Ono [10] and Kocks et al. [7] suggested that p=2/3 and q=2 are suitable values for many metals. Nemat-Nasser et al. [6, 8-9] have demonstrated this fact for several metals. The prediction results for forged Inconel 718 using five sets of p and q values are presented in Figure 3(a). The results revealed the sets of (p=1, q=2) and (p=2/3, q=2) fit well the experimental data. Here, for Inconel 718, Astroloy and Rene 95, we also used the same values for p and q. The parameters k/G_0 and $\dot{\gamma}_r$ characterize the temperature and strain-rate sensitivity of the material. Greater temperature sensitivity is associated with the larger k/G_0, whereas larger $\dot{\gamma}_r$ corresponds to smaller strain-rate sensitivity. However, we did not perform strain rate test, hence, T_c was estimated directly from the experimental data of Figure 3. The procedures are as follows: The experimental data in Figure 3 are obtained by subtracting τ_a, given by Equation (1). It is seen that dynamic strain aging occurs beyond 700K at this strain rate. However, the dynamic strain aging effect was excluded in this model. Some models include dynamic strain aging effect, but it is very complicated [11]. The parameters related to thermal stress in four superalloys are given in Table 2.

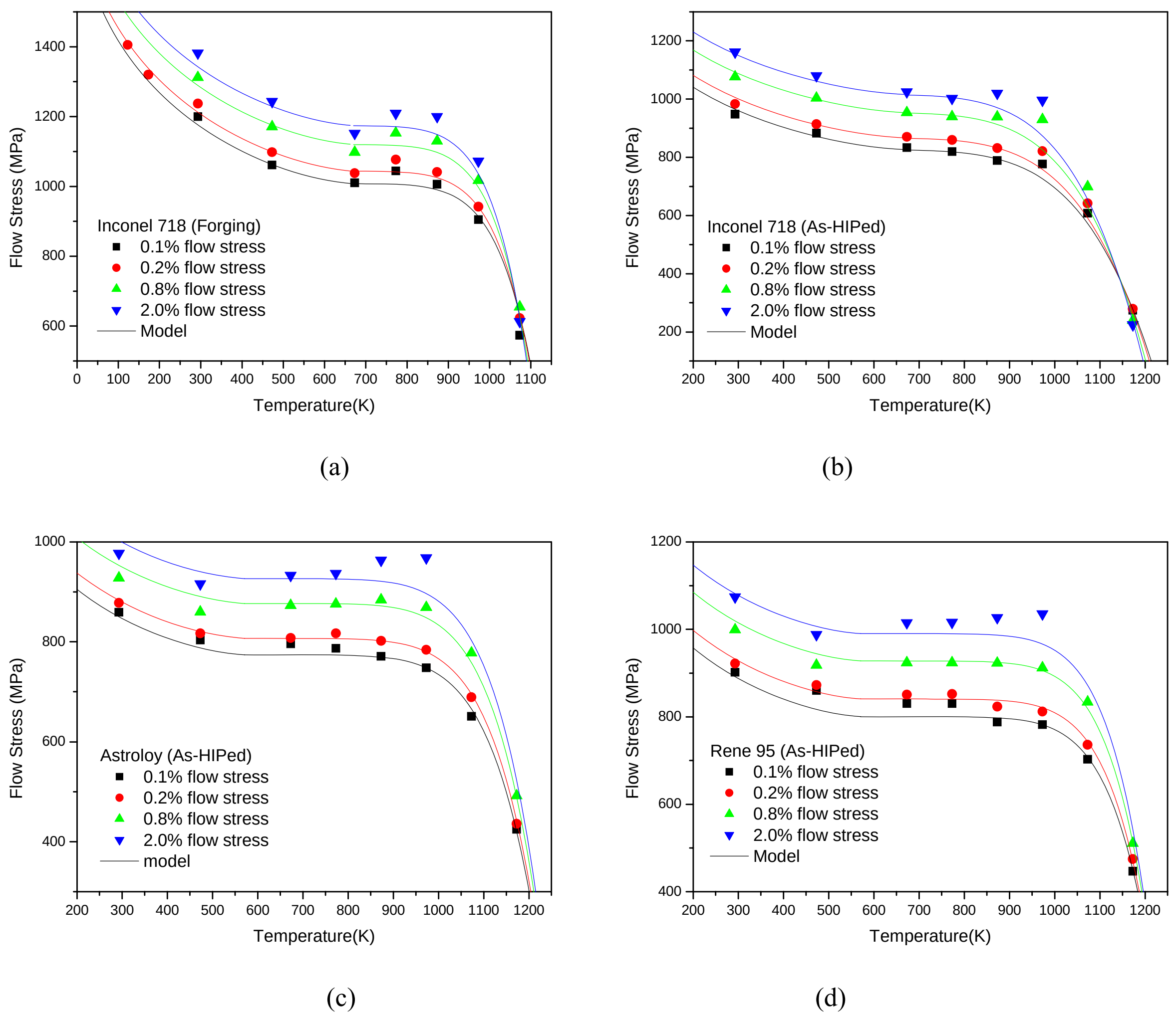

Figure 4: Comparing between the experimental data and the predictions by the model; (a) Inconel 718 made by forging, (b) Inconel 718 made by HIP, (c) Astroloy made by HIP, and (d) Rene 95 made by HIP

4.4 Relaxation component by creep,

As the temperature becomes higher, vacancies percolate to dislocation core and dislocation climb is taken by many vacancies. In this condition, resolved shear stress which is increased by pile-up of dislocation on the slip plane, relaxes. The relaxation stress is related to velocity and density of activated vacancies. The velocity and density of activated vacancies at elevated temperature can be described as follows:

$$\mathbf{v_v = v_0 \exp\left(-Q_v/kT\right)} \quad \mathbf{(8)}$$

$$\boldsymbol{\rho_v = \rho_0 \exp\left(-Q_\rho/kT\right)} \quad \mathbf{(9)}$$

where v_0 and ρ_0 are the mean the initial velocity and the density of activated vacancies, respectively. Also, Q_v and Q_ρ

can be assumed as the activation energies affecting the velocity and density respectively. Relaxation is proportional to the multiplication of this two factors. If the relaxtion follows by the equation of power law creep relationship by dislocation moving,

$$\boldsymbol{\tau_c \propto v_v \rho_v\, \gamma^{n'}\, \dot{\gamma}^{n''}} \tag{10}$$

where n' and n'' are the relaxtion exponent of plastic strain and plastic strain rate respectively. If the temperature in which relaxation arises is assumed to be T_0, and they are also assumed $\tau_c^0 = \alpha v_0 \rho_0\, \dot{\gamma}^{n''}$ and $Q_c = Q_v Q_\rho$, the amount of relaxation is expressed as,

$$\boldsymbol{\tau_c = \alpha v_0 \rho_0\, \gamma^{n'}\, \dot{\gamma}^{n''} \exp\left\{-\frac{Q_v Q_\rho}{k}\left(\frac{1}{T}-\frac{1}{T_0}\right)\right\} = \tau_c^0 \gamma^{n'} \exp\left\{-\frac{Q_c}{k}\left(\frac{1}{T}-\frac{1}{T_0}\right)\right\}} \tag{11}$$

Since we did not performed strain rate dependency tests, τ_c^0 was assumed to consider strain rate effect. It is often said the creep effect arises beyond the temperature $0.3T_m$, however, the temperature for relaxation to arise in this study was found to be $0.5T_m$ in this study. Therefore, T_0 was assumed as $0.5T_m$ and the material constants for the constitutive model were taken as Table 2.
The suggested model predicted well the experimental results in a wide temperature range below 1173K as shown in Figure 4 except some dynamic strain aging regions since the model was not intended to account for dynamic strain aging effect.

Conclusion

For development of high power and light weight liquid rocket engine, hot isostatic pressing (HIP) materials have been used in turbopump system. Uniaxial tensile tests of cylindrical specimens were performed to investigate the flow stress behaviour of forged Inconel 718, HIPed Inconel 718, HIPed Astroloy, and HIPed Rene 95. Based on the physically-based model by Kocks et al., flow stress was derived by both athermal and thermal parts. The suggested model predicted well the experimental data except the dynamic strain aging region; dynamic strain aging occurred in the temperature range from 400 to 700℃ at the strain rate of 0.002/s but its effect was not considered in developling the constitutive model. To expalin the sofening behavior at higher temperatures, creep relaxation effect was also included in the model. With the developed constitutive model, the defomation behaviors of four kinds of superalloys could be described well in the wide range of temperature below 1173K.

Acknowledgements

This research was supported by Korea Aerospace Research Institute in Korea through “Research and Development of Korea Space Launch Vehicle (V)”

References

[1] Alniak, M.O. and Bedir, F. Modeling of deformation and microstructural changes in P/M Rene 95 under isothermal forging conditions. Mater. Sci. Engg. A, 429: 295-303, 2006.
[2] Alniak, M.O. and Bedir, F. Changes in grain size and flow strength in P/M Rene 95 under isothermal forging conditions. Mater. Sci. Engg. B, 130:254-263, 2006.
[3] Guo W-G and Nemat-Nasser, S. Flow stress of Nitronic-50 stainless steel over a wide range of strain rates and temperatures. Mechanics of materials, 38: 1090-1103, 2006.
[4] Hale, C.L., Rollings, W.S. and Weaver, M.L. Activation energy calculations for discontinuous yielding in Inconel 718SPF. Mater. Sci. Engg. A, 300(1-2):153-164, 2001.
[5] Nemat-Nasser, S., Guo, W-G., Nesterenko, V.F., Indrakanti, S.S. and Gu, Y.B., Dynamic response of conventional and hot isostatically pressed Ti-6Al-4V alloys: experiments and modelling. 33:425-439, 2001.
[6] Nemat-Nasser, S. Experimentally-and dislocation-based Multi-scale modelling of metal plasticity including temperature and rate effect. Numisheet, CP778 Volume A:12-19, 2005.
[7] Kocks, U.F., Argon, A.S. and Ashby, M.F. Thermodynamics and kinetics of slip. Prog. Mater. Sci., 19:1-271, 1975.

[8] Nemat-Nasser, S. and Isaacs, J.B. Direct measurement of isothermal flow stress of metals at elevated temperatures and high strain rates with application to Ta and Ta-W alloys. Acta mater., 45(3):907-919, 1997.
[9] Nemat-Nasser, S. and Guo, W-G. Thermomechanical response of DH-36 structural steel over a wide range of strain rates and temperatures. Mechanics of materials, 35: 1023-1047, 2003.
[10] Ono, K. Temperature dependence of dispersed barrier hardening. J. Appl. Phys. 39:1803-1806, 1968.
[11] Cheng, J.Y. and Nemat-Nasser, S. A model for experimentally-observed high-strain-rate dynamic strain aging in titanium. Acta Mater. 48:3131-3144, 2000.

This page has been purposedly left blank